Journal of Medicinal Natural Products

Scilight

Article

In silico Prediction of Anticancer Potential of *Cajanus cajan* (L.) Millsp Phytochemicals as Multi-Target Inhibitors of CTNNB1, BRAF, FGFR and EGFR in Hepatocellular Carcinoma (HCC)

Sibashish Kityania [1], Deepa Nath [2,*], Priyakshi Nath [1], Tamim Ahmed [1], Monjur Ahmed Laskar [3], Satyajit D. Sarker [4], and Anupam Das Talukdar [1,*]

[1] Department of Life Science and Bioinformatics, Assam University, Silchar 788011, India
[2] Department of Botany, Gurucharan University, Silchar 788004, India
[3] Bioinformatics and Computational Biology Centre, Assam University, Silchar 788011, India
[4] Centre for Natural Products Discovery (CNPD), School of Pharmacy and Biomolecular Sciences, Liverpool John Moores University, Liverpool L3 3AF, UK
* Correspondence: dipa.nath@gmail.com (D.N.); anupam@bioinfoaus.ac.in (A.D.T.); Tel.: +91-9435075884 (D.N.); +91-9401416452 (A.D.T.)
Received: 13 October 2025; Revised: 8 January 2026; Accepted: 23 January 2026; Published: 3 February 2026

Abstract: Hepatocellular carcinoma (HCC) is the world's fifth most prevalent malignancy and the second major cause of cancer-related mortality. Although synthetic and plant-based therapies are used to treat a variety of liver illnesses, treatments for HCC are frequently associated with considerable adverse effects as well as drug resistance. Plant-derived natural bioactive compounds, which are known for their low toxicity and protective properties, offer a possibly safer choice for HCC treatment. This study focuses on the most potent plant bioactive compounds for developing new therapeutic alternatives against Hepatocellular carcinoma. A primary phytochemical evaluation was carried out on *Cajanus cajan* (L.) Millsp., exploring both qualitative and quantitative assays and an analysis of its antioxidant properties using DPPH. Metabolites profiling using LC-MS analysis identified 88 phytochemicals from the methanolic extract of the selected plant as bioactive compounds. The HCC molecular target, such as CTNNB1, was identified through the network analysis and BRAF, FGFR and EGFR, were selected based literature study, and their 3D structures were retrieved from the RCSB Protein Data Bank (PDB, https://www.rcsb.org/ (accessed on 12 November 2025). Ligand structures were retrieved from the NCBI PubChem database (https://pubchem.ncbi.nlm.nih.gov/ (accessed on 12 November 2025) and converted into 3D sdf. format for molecular docking analysis. Molegro Virtual Docker (MVD) 6.0 to evaluate the Molecular docking studies considering the interaction between the selected ligands and HCC targets, and compare with positive controls. Among the compounds evaluated, Cis-Mulberroside A, Asperuloside tetraacetate, Rutin, Biorobin and Cassiaside C showed better binding efficiency with the selected targets compared with the positive controls of respective targets. Among these, Cis-Mulberroside A (also referred to as Mulberroside D), a stilbenoid glycoside, exhibited the highest binding affinity for CTNNB1, BRAF, FGFR and EGFR, outperforming the reference compounds. These results suggest that Mulberroside D holds significant inhibitory potential against critical targets in hepatocellular carcinoma (HCC), particularly CTNNB1, BRAF, FGFR and EGFR, which are crucial in the signaling pathways of HCC progression. Based on the phytochemical analysis along with metabolite profiling, Cis-Mulberroside A, stands most prominent bioactive constituent. The molecular docking scores and hydrogen bonding analysis of the selected targets compared to the respective positive control, Cis-Mulberroside A, revealed as a promising compound and could be a potential bioactive phytoconstituent for a valuable drug lead for future use in hepatocellular carcinoma (HCC).

Keywords: *Cajanus cajan* (L.) Millsp; hepatocellular carcinoma (HCC); bioactive compound; LC-MS analysis; Cis-Mulberroside A; molecular docking

1. Introduction

Liver cancer primarily arises directly within the liver and is a significant global health concern. Hepatocellular carcinoma (HCC), the leading form of liver cancer that predominantly occurs in adults [1] and ranks among the most fatal cancers globally, largely because of the frequent delay in diagnosis [2,3]. Although earlier studies highlighted viral hepatitis as the predominant cause of HCC, recent data suggest a shift in etiological patterns, with alcohol consumption and metabolic dysfunction-associated steatotic liver disease (MASLD) [4,5]. The bulletin of the WHO (2020) reported cancer-related deaths include lung cancer, with approximately 1.8 million deaths, followed by colon and rectal cancers at roughly 920,000 deaths, and liver cancer at about 830,000 deaths. Findings reveal that while India's incidence (2.15 per 100,000), prevalence (2.27 per 100,000), and mortality (2.21 per 100,000) rates for HCC are below global averages and these numbers are rising more rapidly in many other countries [6]. Currently, HCC incidence, prevalence, and mortality rates are higher in males, although the rate of increase is notably greater among females [7–9]. According to the GLOBOCAN 2022 report, among men, liver cancer is the fifth highest cause of death from cancer, while it ranks seventh for women globally [10,11]. Each year, more than 850,000 new liver disease cases are reported across the globe, with hepatocellular carcinoma (HCC) constituting 90% of these cases [10,12]. Chemotherapy and radiation treatments often come with adverse side effects, drug resistance, and inefficiency in targeting only cancerous cells, which may also harm healthy tissues. These challenges have prompted increasing interest in alternative therapeutic approaches, particularly those involving natural compounds with potential anti-cancer effects [13,14]. Current treatment methods for liver cancer include psychosocial support, surgical procedures, radiation therapy, chemotherapy, and the use of the receptor tyrosine kinase inhibitor Sorafenib [15].

Sorafenib, a multi-kinase inhibitor (TKI), was approved to treat advanced hepatocellular cancer, along with metastatic renal cell cancer (RCC) and well-differentiated radioiodine-resistant thyroid cancer (DTC) [16–18]. The multi-kinase inhibitor regorafenib was analysed in advanced HCC after sorafenib and showed greater efficacy [19]. Lenvatinib is a multi-tyrosine kinase inhibitor that targets VEGFR1–3, RET and FGFR1–3, but these drugs showed side effects such as weight loss, hypertension, diarrhoea and fatigue [20–23]. Patients with HCC using these conventional medications have also seen toxic effects in their spleen and thymus in addition to the liver [24]. TCGA data indicate that about 27% of HCC cases carry gain-of-function mutations in CTNNB1, the gene encoding β-catenin. These mutations—mainly within exon 3—disrupt normal phosphorylation-dependent degradation, allowing β-catenin to accumulate and drive unchecked transcriptional activity [25,26]. EGFR is discovered to be highly expressed in both human cirrhotic liver tissues and hepatocellular carcinomas (HCCs). Increased expression of EGFR ligands, such as TGF-α, EGF, HB-EGF, amphiregulin (AR), and betacellulin (BTC), along with the enzyme ADAM17, has also been noted in liver tumor cells and tissues [27,28].

Plant-derived bioactive metabolites contain anti-cancer, anti-inflammatory, and antioxidant properties, making them useful for the prevention and treatment of various disorders [29]. Prominent ethnomedicinally potential plants also exhibiting bioactivity across various new therapeutic models, thus plant-derived natural products remain a potent reservoir of vital phytocompounds with healing properties [15,30–33]. Due to their minimal adverse effects, herbal remedies as anticancer agents are gaining popularity as these composites have been explored to suppress the progression of multiple cancers by affecting cell proliferation, interfering with multiple signaling pathways, and downregulating the major gene expression [15,32–34]. Nevertheless, bioactive compounds from natural sources have the potential to neutralize ROS (reactive oxygen species) and strong tendency to donate electrons to stabilize free radicals, helping to prevent cellular damage [3,14,35]. The pigeon pea (*Cajanus cajan* (L.) Millsp.) from the Family: Fabaceae, is a significant legume in tropical regions, and emerging research highlights its numerous health benefits [36,37].

The metabolic profiling of *Cajanus cajan* (L.) Millsp compounds are playing a significant role in advancing and optimizing and improving Liver cancer treatment strategies. As a result, discovering novel therapeutic strategies for Liver cancers like Hepatocellular carcinoma (HCC) has become a key focus in modern research. While various bioactive components of *C. cajan* leaves, seeds, and roots have been studied, detailed comparative data on their fundamental nutritional profiles and biological activities remain limited. Therefore, our study focused on the leaf extract and its phytochemicals to identify potential anti-HCC candidates for future drug development. Employing computational predictions and Molecular docking analysis, this research evaluates their potential as anti-HCC agents.

2. Methodology

2.1. Collection of Plants

In October, the fresh leaves of *Cajanus cajan* (L.) Millsp were gathered from their natural environment in the campus of Assam University, Silchar (Latitude 24.686748°, Longitude 92.751486°), Cachar district of Southern

Assam, Northeast India and submitted to Assam University Silchar Central Herbarium (AUSCH) for identification with voucher Number—*S. Kityania 1*, Accession Number—AUSCH 8560. The recognition of these species was validated by contrasting them with examples that already exist at the Assam University Herbarium in Silchar, Assam.

2.2. Preparation of Plant Extract

The plant materials were initially cleaned and air-dried, then ground into powder for extraction with solvents of progressively increasing polarity. Using a maceration technique, the dried plant powder was sequentially soaked in petroleum ether, ethyl acetate, acetone, and methanol. Each extraction lasted for 72 h with intermittent shaking. After extraction, the filtrates were concentrated by removing the solvents entirely and were then used in further experiments for both qualitative and quantitative phytochemical analyses [38].

2.3. Phytochemical Analysis of the Selected Plants

2.3.1. Qualitative Phytochemical Analysis

Preliminary Phytochemical analysis was done on the extracts of petroleum ether, ethyl acetate, acetone, and methanol from each plant to assess the presence or absence of various bioactive phytochemical compounds as outlined below. The plant extracts derived from the chosen plants were analyzed through initial phytochemical screening to determine which bioactive chemicals are present, including phenols, alkaloids, flavonoids, saponins, and tannins [39]. The list of chemicals and reagents is listed in the supplementary file 1.

Phenol

To test for phenolic compounds in the extract, 50 mg of the extract was dissolved in distilled water, and then 3 mL of a 10% lead acetate solution was added. The formation of a large white precipitate confirms the appearance of phenols [40,41].

Alkaloids

The plant extract in a beaker was heated in a water bath while a 2% HCl solution was added. Mayer's reagent was added dropwise to the mixture after it had cooled and been filtered. The presence of alkaloids was revealed by the development of turbidity or yellow precipitate [39,42].

Flavonoids

A test tube was set up with 1.5 mL of a 50% methanol solution, to which 4 mL of a plant extract was introduced. Magnesium metal was added to the mixture while gently heating it. Five to six drops of strong hydrochloric acid were then added. Flavones were suggested by an orange hue, while flavonoids were indicated by the development of a red colour [43,44].

Saponins

An extract weighing 1 g was combined with 5 milliliters of distilled water in a test tube and boiled. After filtering the mixture, adding three milliliters of distilled water to the filter, the mixture was violently agitated for five minutes. The presence of saponins is confirmed by the formation of persistent foam during heating [45].

Tannins

A solution was prepared by mixing 0.5 g of extract with 10 mL of distilled water, which was then filtered. A few drops of 1% $FeCl_2$ were added to 2 milliliters of the resultant filtrate; the presence of tannins is indicated by the formation of a green, blue-green, or blue-black precipitate [46,47].

2.3.2. Quantitative Phytochemical Analysis

Estimation of Total Phenolic Content (TPC)

To assess the TPC of the plant extract, a standard protocol was employed [48,49]. A 500 µL aliquot of the extract at a concentration of 1 mg/mL in methanol was placed in a test tube, followed by the addition of 100 µL of Folin–Ciocalteu reagent and 2400 µL of distilled water. After allowing the mixture to sit for 3 min, 2000 µL of a 2% sodium carbonate (Na_2CO_3) solution was incorporated. After an hour of dark incubation, the mixture's absorbance at 750 nm was measured. The findings were reported as gallic acid equivalents (GAE/mg) of the plant extract.

Estimation of Total Flavonoid Content (TFC)

The total TFC was quantified using a standard method [50,51]. A 1000 μL aliquot of the extract, prepared at a concentration of 1 mg/mL in methanol, was combined with an equal volume of 2% aluminum chloride solution (also in methanol). The absorbance at 415 nm was measured after this combination was incubated for 15 min in the dark. The outcomes were disseminated as the equivalent amount of quercetin (QE/mg) in the plant extracts analyzed.

2.4. Antioxidant Activity

DPPH Free Radicals Scavenging Activity

The antioxidant profiling of the extracts was evaluated by their ability to scavenge DPPH free radicals following the established procedure [52,53]. Initially, a 1 mg/mL stock solution was prepared and then diluted in methanol to achieve five varying concentrations. Each diluted extract (2 mL) was combined with 2 mL of an 80 μg/mL DPPH methanol solution and allowed to sit in the dark for 30 min. The absorbance at 517 nm was measured for the mixture. The control sample included DPPH mixed with methanol alone, excluding the extracts. Ascorbic acid was used as a reference standard for comparison. An IC_{50} value for each extract was determined by creating a concentration-response curve, and the percent inhibition was calculated using the formula provided.

$$\text{Free radical scavenging (\%)} = A_C - A_t/A_C \times 100$$

Free radical scavenging, whereas the absorbance of the test sample is denoted by A_t and the absorbance of the control by A_C.

2.5. Antioxidant Enzyme Estimation

The following steps were taken to assess the antioxidant enzyme activity in the plant extracts.

2.5.1. Preparation of Plant Extract for Antioxidant Enzyme Tests

To assess the activities, a 100 mg sample of the extract was incorporated with ice-cold potassium phosphate buffer (pH 6.8, 0.1 M) containing 1% polyvinyl pyrrolidone (PVP), 0.1 mM phenylmethanesulfonyl fluoride (PMSF), and 0.1 mM ethylenediaminetetraacetic acid (EDTA). The mixture was extensively processed using a pre-chilled mortar and pestle. After homogenization, the mixture was centrifuged at 13,000 rpm for 15 min at 4 °C to extract the supernatant, which was then used for the enzyme tests [54,55].

2.5.2. Catalase (CAT) Assay

Catalase (CAT) activity was determined by measuring absorbance at 240 nm, which indicates the reduction in H_2O_2 concentration. The assay mixture contained 0.5 mL of enzyme extract, 15 mM H_2O_2, and 0.5 mL of 0.1 M phosphate buffer at pH 6.8. Absorbance at 240 nm was recorded within one minute after the enzyme was added [56,57].

2.5.3. Superoxide Dismutase (SOD) Assay

The activity of SOD was evaluated by its capacity to hinder the photochemical reduction of Nitroblue tetrazolium (NBT). In this assay, 0.2 mL of enzyme extract was mixed with 2.5 mL of phosphate buffer (pH 6.8), 0.1 mL of bovine serum albumin (BSA) at a concentration of 3.3×10^{-3}%, 0.1 mM riboflavin, and 6 mM NBT. The reaction mixture was then illuminated for 10 min, and the reaction rate was quantified by measuring absorbance at 560 nm with an Eppendorf UV-visible spectrophotometer [58,59].

2.6 Sample Preparation

In preparing samples for LC-MS, 50 mg of dried extract was disintegrated in 1 mL of methanol and subsequently filtered using a nylon membrane filter.

2.7. Liquid Chromatography-Mass Spectrometry (LC-MS)

IIT Bombay's SAIF, using Varian Inc.'s (Palo Alto, CA, USA) 410 Prostar Binary LC with 500 MS IT PDA Detectors, was used for LC-MS analysis was conducted. The High-Resolution Liquid Chromatography (HRLC) analysis was conducted using an HRLC instrument from Agilent Technologies (Santa Clara, CA, USA). The extract was reconstituted in an 80:20 solution of acetonitrile and water, containing 0.1% formic acid, to achieve a

final concentration of 1 mg/mL. After that, this solution was centrifuged at 10,000 g for 10 min to eliminate any residual particles.

Separation of the components was carried out on an RRHT C18 column with dimensions of 2.1 mm in diameter, a length of 100 mm, and a particle size of 1.8 μm.

The mobile phase consists of two solvents: Solvent A, a mixture of water with 0.1% formic acid (FA). Solvent B, a mixture of acetonitrile containing 10% water and 0.1% formic acid. A flow rate of 0.300 mL/min and an injection volume of 5 μL were applied. The column was maintained at a temperature of 40 °C. This method was used for analyzing both standard compounds and sample extracts. The solvent composition used in the procedure is shown in Table 1.

To achieve optimal gradient elution, the parameters shown in Table 2 were implemented.

Table 1. Composition of solvent for the LC-MS analysis.

SL No.	Channel	Ch.1 Solv.	Name 1	Ch.2 Solv.	Name 2	Selected	Used	Percent
1	A	100.0% Water V.02	0.1% FA in water	100.0% Water V.02		Ch.2	Yes	95.00%
2	B	100% Methanol V. 03	90% CAN + 10% + H2O + 0.1% FA	100.0% Acteonitrile V. 02		Ch. 2	Yes	5.00%

Table 2. The precise duration and solvent gradient profile utilized in the LC-MS procedure.

SL No.	Time	A	B	Flow	Pressure
1	1.00 min	95.00%	5.00%	0.300 mL/min	1200.00 bar
2	25.00 min	0.00%	100.00%	0.300 mL/min	1200.00 bar
3	30.00 min	0.00%	100.00%	0.300 mL/min	1200.00 bar
4	31.00 min	95.00%	5.00%	0.300 mL/min	1200.00 bar
5	35.00 min	100.00%	00.00%	0.300 mL/min	1200.00 bar

The mass spectrometry (MS) analysis utilized an Agilent G6550A Q-TOF MS system with a Dual AJS ESI ion source. An absorbance threshold of 200 was established for MS, while MS/MS had a threshold of 5. Both MS and MS/MS scan rates were configured at 1.00 spectra per second, with a medium isolation width of about 4 amu for MS/MS. The MS range spanned from a minimum of 150 m/z to a maximum of 1000 m/z.

The MS Conditions were applied in the procedure as follows:

Component Model: G6550A, Component Name: MS Q-TOF, Source of Ion: Dual AJS ESI, MS Absorbance threshold: 200, MS/MS Absorbance threshold: 5, MS/MS Scan Rate (spectra/sec): 1.00, Isolation Width MS/MS: Medium (~4 amu), MS Scan Rate (spectra/sec): 1.00, Min MS Range (m/z): 150, Max MS Range (m/z): 1000.

2.8. Analysis of Gene Interaction Networks in Hepatocellular Carcinoma (HCC)

Analysis of gene networks was done to pinpoint the key genes involved in HCC, potentially identifying targets that could be addressed with drug therapies.

2.8.1. Retrieval of HCC-Associated Genetic Factors

A collection of 4111 genes connected with human hepatocellular carcinoma (HCC) was acquired from the NCBI Gene database (https://www.ncbi.nlm.nih.gov/gene/ (accessed on 12 November 2025).

2.8.2. Protein-Protein Interaction (PPI) Network

The STRING database version 12.0, a tool designed for predicting protein-protein interactions, was utilized in this analysis. Given that the database can process a maximum of 2000 genes at once, Funrich software v.3.1.3 was employed to filter the dataset to the top 1500 most significant genes. STRING generates biologically relevant associations using multiple forms of evidence, including mining of scientific literature, experimental results, curated databases, shared selective signals across various genomes, systematic co-expression analyses, and knowledge exchanges based on gene ontology from numerous species. For this study, a threshold of 0.900 was set for the confidence score, proving that forecasts with higher scores are more reliable [60].

2.8.3 Clustering of Genes

To analyze the extensive gene network, we utilized the Molecular Complex Detection application (MCODE) from Cytoscape 3.8.2 to identify highly interactive regions, referred to as clusters. These clusters are prioritized

according to MCODE scores, which are determined by assessing the density of the nodes and the proportion of the edges [61,62].

2.8.4. Functional Enrichment Analysis

Functional enrichment analysis has been employed to determine significant clusters, potentially influencing disease characteristics. Subsequently, identified clusters were examined using DAVID (Database for Annotation, Visualization and Integrated Discovery) Bioinformatics resources (https://david.ncifcrf.gov/ (accessed on 17 November 2025), a functional annotation tool that interfaces with the OMIM Disease database to identify human disease-related genes from all the clusters produced by MCODE analysis [63].

2.9 Molecular Docking Analysis

Molecular docking analysis was done using the Molegro Virtual Docker 6.0 (MVD) software (Molexus ApS, Aarhus, Denmark) to precisely predict how ligands bind and orient themselves within the active sites of receptors. Upon importing the receptors into MVD, previously bound inhibitors and water molecules were eliminated, and the protonation states of the amino acids were modified as necessary. The identification of the active sites was accomplished through MVD's cavity detection feature, which delineated the docking locations. After Energy minimization and optimization of hydrogen bonds, the software generated the MolDock score, hydrogen bond score, and determined the optimal geometry for ligand binding at the active site(s) of the receptor [64,65].

The protein selected for the molecular docking analysis is detailed in Table 3.

Table 3. The target protein utilized in the molecular docking study (Receptor information retrieved from the RCSB PDB database, https://www.rcsb.org/ (accessed on 12 November 2025).

Sl No.	Receptor	PDB ID	R-free	Resolution	Experimental Methods
1	CTNNB1	1LUJ	0.255	2.50 Å	X-RAY DIFFRACTION
2	BRAF	4E26	0.262	2.55 Å	X-RAY DIFFRACTION
3	FGFR1	4V04	0.228	2.12 Å	X-RAY DIFFRACTION
4	EGFR	6DUK	0.223	2.20 Å	X-RAY DIFFRACTION

3. Results

3.1. Phytochemical Analysis of Cajanus cajan (L.) Millsp. Extracts

The Herbarium of the plant was submitted to Assam University Central Herbarium (AUSCH) with voucher Number—*S. Kityania 1*, Accession Number—AUSCH 8560.

The initial qualitative phytochemical analysis of the plant extracts identified the presence of several secondary metabolites that include phenols, alkaloids, flavonoids, saponins, and tannins. The total phenolic content and flavonoid concentration analysis of the selected plants indicate that *Cajanus cajan* (L.) Millsp. exhibits a higher phenolic concentration in its methanolic extract. Among the various *Cajanus cajan* (L.) Millsp. extracts tested against DPPH radicals, the methanolic extract emerged as the most effective, surpassing the petroleum ether, ethyl acetate, and acetone extracts. This extract recorded an IC50 value of 358.93 µg/mL, indicating substantial activity, though not as strong as that of the standard ascorbic acid (IC50, 213.27 µg/mL). The preliminary phytochemical analysis of the extract has been provided in the Supplementary File 1. (A comprehensive summary of qualitative analysis shown in Table S1 and bar diagram of the TPC, TFC, DPPH, CAT and SOD results is shown in the accompanying Supplementary Figures S1–S7.)

3.2. Metabolite Profiling: LC-MS (Liquid Chromatography Mass Spectroscopy) Analysis

Based on the studies and the obtained results from phytochemical screening were further analysed using the LC-MS of the methanolic extract of *Cajanus cajan* (L.) Millsp. LC-MS analysis was conducted at IIT Bombay's SAIF using Varian Inc.'s (Palo Alto, CA, USA) 410 Prostar Binary LC with 500 MS IT PDA Detectors. Chromatogram of LC-MS analysis of *Cajanus cajan* (L.) Millsp. (Methanolic extract) shown in Figure 1 and the list of identified compounds is shown in Tables 4 and 5. The fragmentation pattern and details of the listed compounds are given in the supplementary files 2 & 3, respectively, for both Tables 4 and 5.

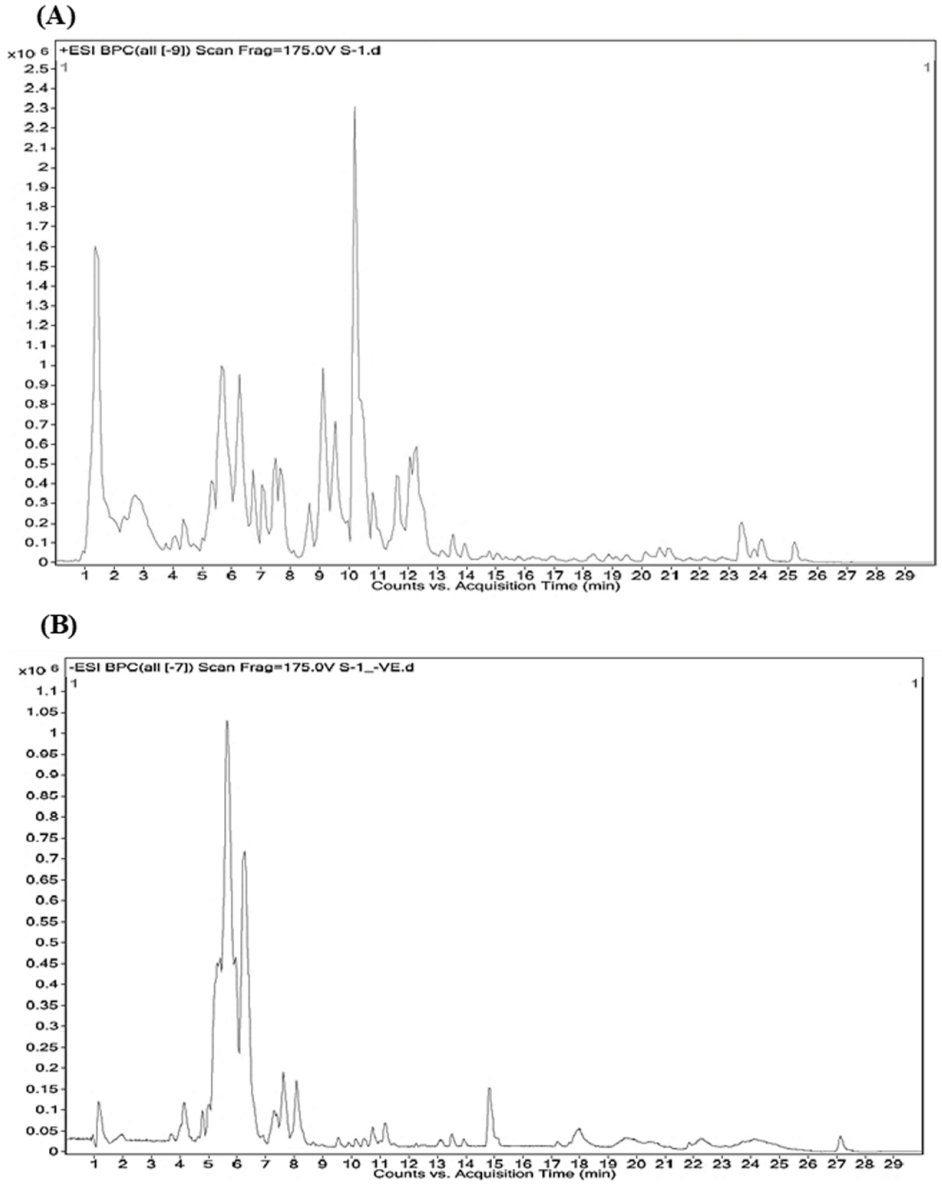

Figure 1. (**A**) Chromatogram of LC-MS of Methanolic extract of *Cajanus cajan* (L.) Millsp. in Positive (+ve)-polarity modes of electrospray ionization (ESI) mass spectrometry. (**B**) Chromatogram of LC-MS of Methanolic extract of *Cajanus cajan* (L.) Millsp. in Negative (-ve)-polarity modes of electrospray ionization (ESI) mass spectrometry. (Highlighted and mentioned the compound name of some major peaks in both the chromatograms).

Table 4. The table below presents the phytocompounds identified through LC-MS analysis performed in positive ESI mode of *Cajanus cajan* (L.) Millsp.

SL No.	Name	Score	Mass	m/z	RT
1	3beta,6beta-Dihydroxynortropane	96.2	143.0943	144.1014	1.158
2	Lentiginosine	86.93	157.1099	158.1172	1.251
3	Indospicine	82.29	173.1162	174.1234	1.529
4	Pirbuterol	98.95	240.1473	241.1545	1.598
5	2-Nitroanisole	97.11	153.0424	154.0495	2.225
6	Actinidine	87.4	147.1047	148.112	2.642
7	O-7-Angelylheliotridine	90.32	237.1364	238.1438	3.698
8	Pinacidil	89.39	245.1625	246.1698	4.008
9	Tanakine	84.65	219.1258	220.1332	4.009
10	Aspergillic acid	65.9	224.1548	247.1439	4.23
11	Feruloylputrescine	84.85	264.1474	265.1547	4.545
12	(20S)-20-Hydroxypregn-4-en-3-one	91.44	316.2386	339.2278	4.701
13	Rheinoside A	97.46	610.1541	611.161	4.718

Table 4. *Cont.*

SL No.	Name	Score	Mass	m/z	RT
14	Crotamiton	75.73	203.1305	204.1381	4.871
15	4Z,7Z,10Z-octadecatrienenitrile	83.75	259.2281	282.2175	4.943
16	Oxprenolol	64.56	265.1673	266.1751	4.944
17	Biorobin	96.82	594.1594	595.1665	5.022
18	Farnesylcysteine	51.49	325.2115	348.2015	5.244
19	Rustoside	98.86	580.1436	581.1509	5.324
20	Europine	90.93	329.1839	330.1908	5.471
21	Ibopamine	75.66	307.178	308.1856	5.538
22	Kaempferol 3-rhamnoside 7-xyloside	98.92	564.1485	565.1557	5.603
23	6″-O-Malonylwistin	98.37	546.1377	547.1449	5.609
24	(+)-Mahanimbicine	40.8	331.1986	332.2062	5.76
25	Mahuannin D	52.03	528.1503	551.1394	5.831
26	Meperidine (pethidine)	86.54	247.157	248.1642	5.905
27	3-(4-Hydroxy-3-methoxyphenyl)-1,2-propanediol 2-O-(galloyl-glucoside)	79.72	512.1563	535.1456	6.12
28	Inundatine	95.05	261.1728	262.1801	6.297
29	Formononetin 7-(6″-malonylglucoside)	99.23	516.1272	517.1345	6.362
30	Lophocerine	99.39	249.1729	250.1802	6.514
31	Fabianine	99.2	219.1626	220.17	6.682
32	Mesembrinol	85.75	291.1837	292.191	7.054
33	Capsaicin	79.31	305.1988	306.2062	7.251
34	5-Hydroxy-3,3′,7,8-tetramethoxy-4′,5′-methylenedioxyflavone	94.97	402.0955	403.1025	7.287
35	N-(Cyclohexylmethyl)-N-methylbenzenamine	99.09	203.1671	204.1743	7.374
36	Halocins	25.73	305.1809	306.1882	7.41
37	alpha-Eucaine	85	333.194	334.2014	7.53
38	Cardiopetalidine	89.3	363.2414	364.2485	8.594
39	2-Phenylethyl 3-methylbutanoate	87.24	206.1306	207.1379	8.605
40	3-buten-2-one 1-(2,3,6-trimethyl phenyl)	85.05	188.1198	189.1271	8.638
41	Dihydrocapsaicin	92.16	307.2145	308.2223	8.992
42	Tolterodine	6.66	325.2459	348.2351	9.358
43	Icaceine	96.39	375.2417	376.2489	9.47
44	4-Methyl-4-aza-5-pregnene-3,20-dione	82.68	329.2379	352.227	10.051
45	Dihydrodeoxystreptomycin	80.13	567.29	568.297	10.207
46	Hypercalin B	75.35	518.3015	519.3067	10.223
47	Borrelidin	95.11	489.3094	490.3169	10.445
48	Istamycin C	46.11	403.2728	404.2796	10.837
49	Salmeterol	80.7	415.2751	438.2641	11.714
50	Gymnodimine	99.05	507.335	508.3422	11.941
51	23-Acetoxysoladulcidine	99.68	473.3506	474.358	12.024
52	2-(3-Phenylpropyl) tetrahydrofuran	98.94	190.1354	191.1426	12.502
53	7b-Hydroxy-3-oxo-5b-cholanoic acid	95.49	390.2777	391.2848	23.359

Table 5. The table below presents the phytocompounds identified through LC-MS analysis performed in negative ESI mode of *Cajanus cajan* (L.) Millsp.

SL No.	Name	Score	Mass	m/z	RT
1	2,4-Dichloro-3-oxoadipate	64.06	227.959	272.9572	0.935
2	L-Arabinose	93.4	150.0518	149.0445	1.168
3	Nitecapone	68.66	265.0611	264.0541	1.774
4	Dihydrocaffeic acid 3-O-glucuronide	96.15	358.0897	403.0877	3.649
5	Fenitropan	70.37	281.0925	280.0855	4.256
6	Asperuloside tetraacetate	98.39	582.1582	581.1511	4.579
7	Rutin	98.06	610.1534	609.1461	4.678
8	Cassiaside C	87.27	596.1735	595.1664	4.766
9	5′-Hydroxycastavinol	98.15	566.1632	565.156	4.957
10	Rustoside	43.26	580.1466	579.135	4.964
11	Quercetin 3,7-dirhamnoside	89.84	594.1587	593.151	5.009
12	Ephedrannin A	41.34	556.0963	615.1115	5.22
13	Diosmetin 7-O-beta-D-glucuronopyranoside	99.48	476.0955	475.0882	5.256
14	Salviaflaside methyl ester	98.22	536.1529	535.1455	5.519

Table 5. *Cont.*

SL No.	Name	Score	Mass	m/z	RT
15	Kaempferol 3-rhamnoside 7-xyloside	96.72	564.1491	563.1418	5.621
16	Irisolidone 7-O-glucuronide	96.59	490.1115	549.1252	5.776
17	8-C-Galactosylluteolin	99.62	448.1005	447.0932	5.837
18	Phrymarolin I	53.67	488.1341	533.1301	5.849
19	Genistein 8-C-glucoside	87.74	432.1065	431.0988	6.274
20	Cassiaside	98.76	404.1106	403.1034	6.803
21	Lippioside I	95.49	538.1681	537.1608	6.933
22	cis-Mulberroside A	98.28	568.179	567.1719	7.287
23	5-Hydroxy-3,3′,7,8-tetramethoxy-4′,5′-methylenedioxyflavone	86.25	402.0955	401.0877	7.318
24	Polyethylene, oxidized	84.79	244.1305	243.1232	7.591
25	Ethiprole	47	395.9792	394.9717	7.667
26	Neoastilbin	98.56	450.1163	449.1091	7.718
27	Astringin	81.7	406.1265	405.1192	7.766
28	Pyrazosulfuron-ethyl	90.17	414.0958	459.0931	7.965
29	6-Feruloylcatalpol	96.6	538.1689	537.1617	8.034
30	Oroxindin	95.06	460.1006	459.0931	8.307
31	Ipomeatetrahydrofuran	98.36	256.204	301.2021	10.727
32	Kessyl glycol	84.84	254.1883	299.1866	11.136
33	8-Acetoxy-4-acoren-3-one	97.02	278.1874	277.1802	14.82
34	Lauryl hydrogen sulfate	93.25	266.1547	265.1475	17.791
35	Canrenone	77.26	340.2062	339.1994	23.774

3.3 In silico Prediction of Bioactivity of Potential Phenolics

3.3.1. Network Analysis of Genes and Identification of Potential Drug Targets for Hepatocellular Carcinoma (HCC)

The NCBI Gene database obtained a dataset of 4111 genes connected with human hepatocellular carcinoma (HCC). FunRich software v3.1.3 was used to select the top 1500 genes. These genes' protein-protein interactions (PPI) (Shown in Figure 2) were then analyzed using the STRING database v12.0 with a confidence score threshold of 0.900 for the highest accuracy. The database generated a network of 1438 nodes out of 1500 genes and a total number of 18,267 edges.

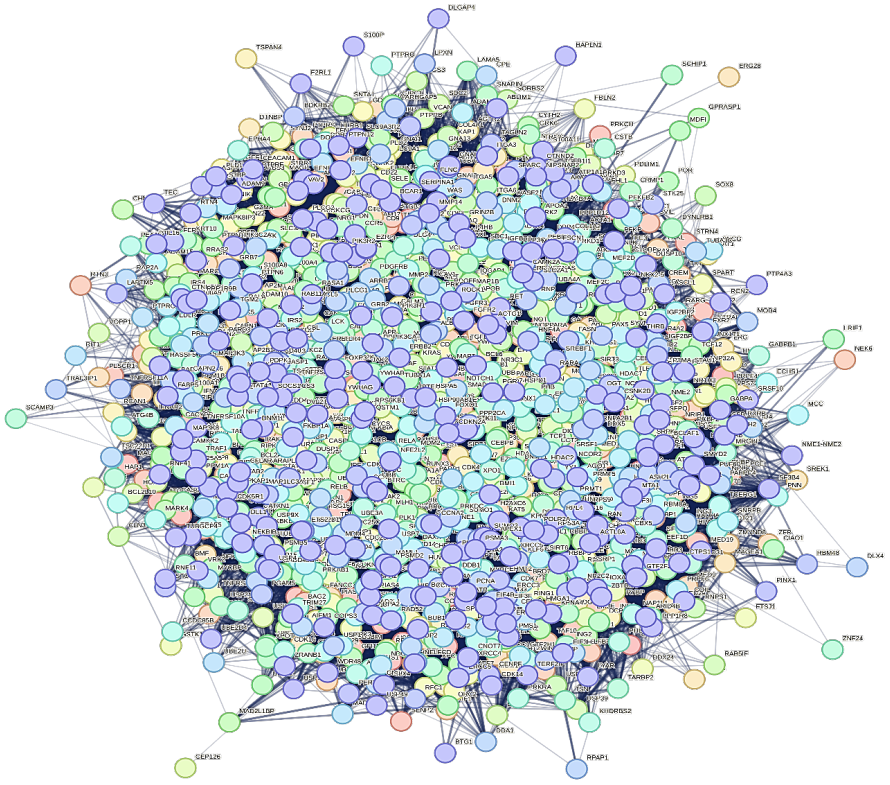

Figure 2. The String web server created a protein-protein interaction (PPI) network of the top 1500 hepatocellular carcinoma (HCC) genes.

3.3.2. Selection of Gene Clusters

Using the MCODE app in Cytoscape, clusters within the network were identified as regions with high interconnectivity. In this analysis, a total of 20 gene clusters were detected and ranked as the app's default settings. Every cluster was investigated in further detail with the DAVID Bioinformatics tool, focusing on the OMIM Disease database for functional annotation. The analysis found that only two clusters had links to human diseases, while the remaining 18 clusters did not show associations with HCC. Specifically, disease-related genes were identified in clusters 4 and 9, with four genes showing strong associations with HCC: AXIN1 and CASP8 in Cluster 4, and CTNNB1 and TP53 in Cluster 9. In our study aimed at inhibiting oncogenes to prevent HCC, we chose CTNNB1 as the primary focus for further research, as it functions as an oncogene. The other three genes considered—AXIN, CASP8, and TP53—are classified as tumor suppressor genes. Figure 3A,B shows the clusters that are associated with HCC.

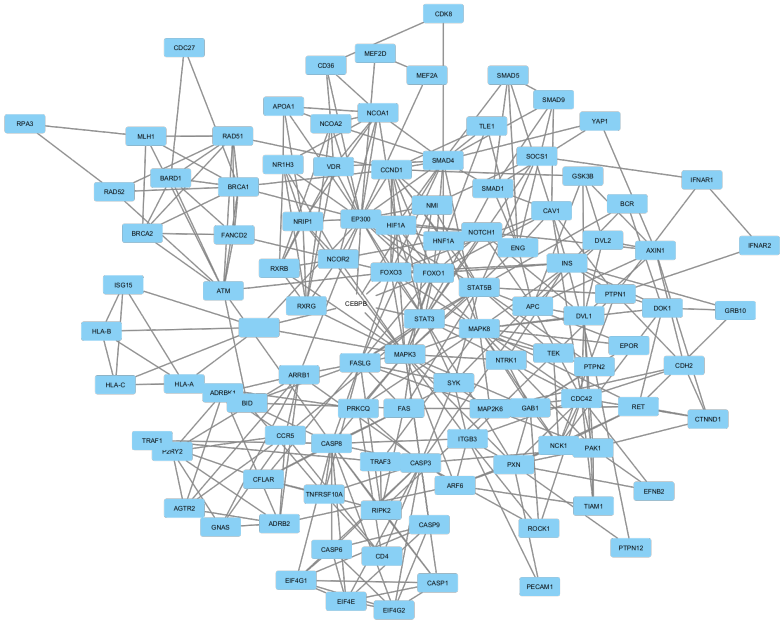

(A)

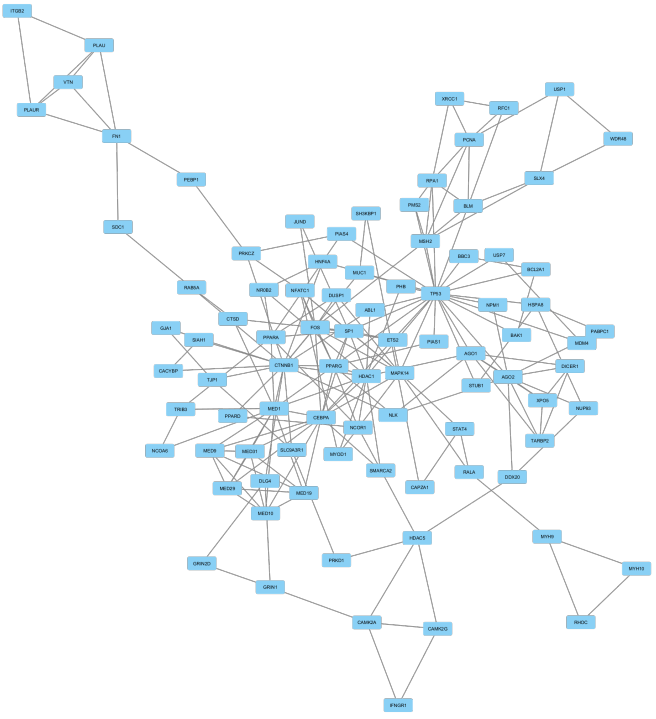

(B)

Figure 3. (**A**): Cluster 4 generated using the MCODE app in Cytoscape; (**B**): Cluster 9 generated using the MCODE app in Cytoscape.

The literature search for targets and KEGG pathway analysis for hepatocellular carcinoma (HCC), 3 additional target proteins, along with CTNNB1, were identified for their relevance in HCC treatment. The employed targets are as follows: CTNNB1 (PDB ID: 1LUJ), BRAF (PDB ID: 4E26), FGFR1 (PDB ID: 4V04), EGFR (PDB ID: 6DUK).

3.4. Molecular Docking Analysis: Binding Affinities and Receptor Inhibition Analysis

All compounds identified via LC-MS, the compounds were selected for molecular docking analysis.

Docking Score and Inhibition of Receptors

Through gene network analysis, CTNNB1 was identified as the most influential gene associated with liver cancer. Additionally, literature reviews highlighted other significant genes, which include FGFR1, BRAF, and EGFR. Molecular docking analysis revealed that, among all the identified compounds, Cis-Mulberroside A, Asperuloside tetraacetate, Rutin, Biorobin and Cassiaside C showed better binding efficiency with the selected targets compared with the positive controls of respective targets. Cis-Mulberroside A demonstrated the highest binding efficiency with these drug targets. Summarizes the docking scores (MolDock score) and hydrogen bonding interactions for the top three compounds, along with their reference positive control, shown in Table 6. Figures 4 and 5 show the 3D pose and 2D interactions of the respective controls with selected targets, respectively and Figure 6 display the 3D docking pose & Figure 7 shows the 2D docking poses for Cis-Mulberroside A with the targets. Figure 8 shows the Chemical Structure of all 5 top compounds for all the targets and the Details of the key binding residues of various interactions of the targets with Cis-Mulberroside A are summarizes in Supplementary file 1—Table S2.

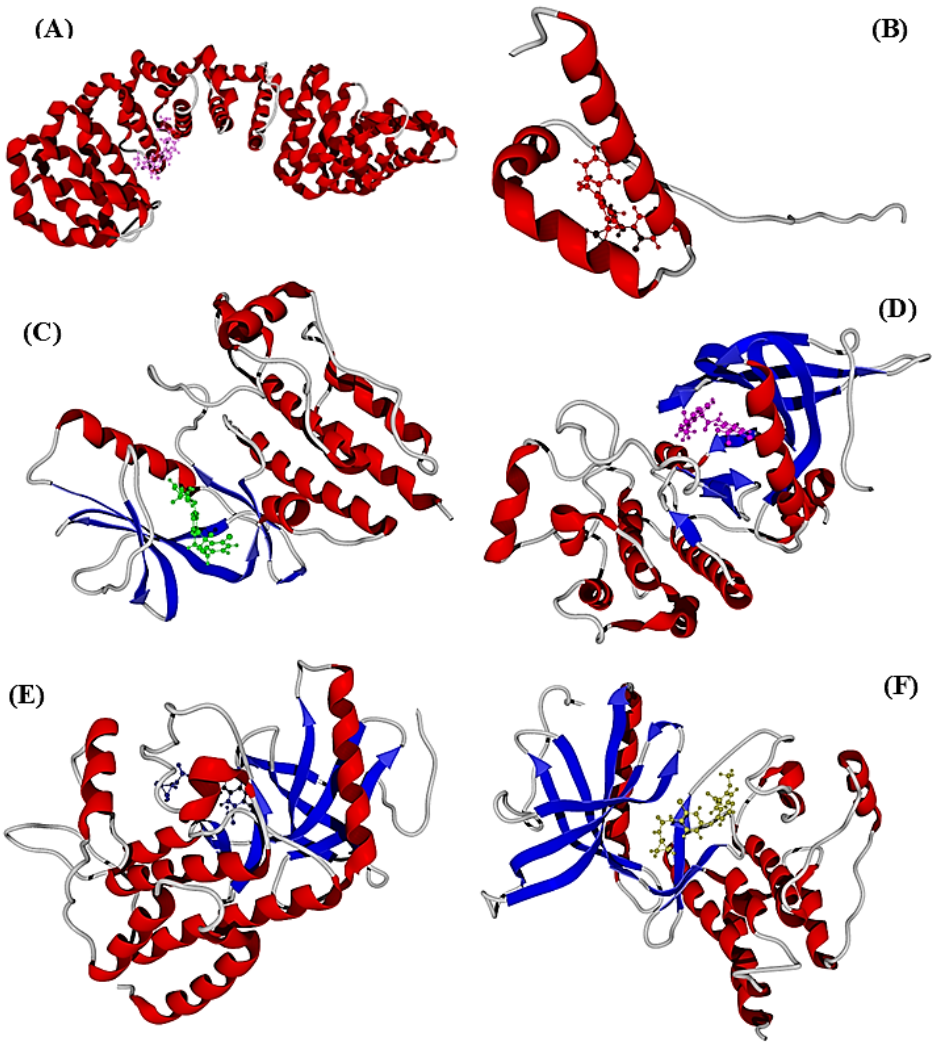

Figure 4. Docking pose of positive controls with different targets (Where, (**A**): Trametinib with CTNNB1 Chain 1; (**B**): Trametinib with CTNNB1 Chain 2; (**C**): Regorafenib with BRAF Chain 1; (**D**): Lenvatinib Mesylate with EGFR Chain; (**E**): Lenvatinib Mesylate with FGFR1 Chain 1; (**F**): Lenvatinib Mesylate with FGFR2 Chain 2).

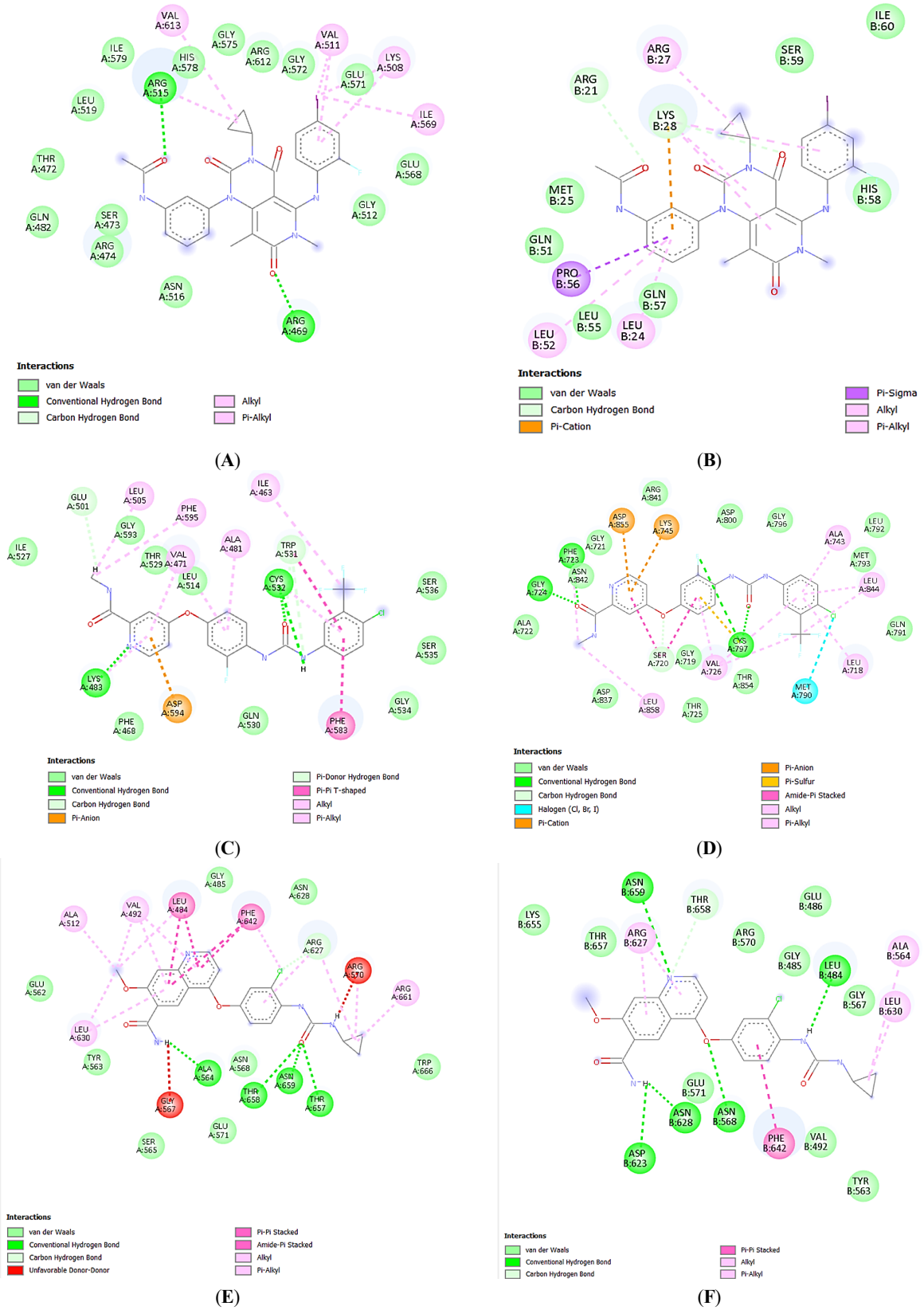

Figure 5. Docking interaction of positive control with different targets (Where, (**A**): Trametinib with CTNNB1 Chain 1; (**B**): Trametinib with CTNNB1 Chain 2; (**C**): Regorafenib with BRAF Chain 1; (**D**): Lenvatinib Mesylate with EGFR Chain; (**E**): Lenvatinib Mesylate with FGFR1 Chain 1; (**F**): Lenvatinib Mesylate with FGFR2 Chain 2).

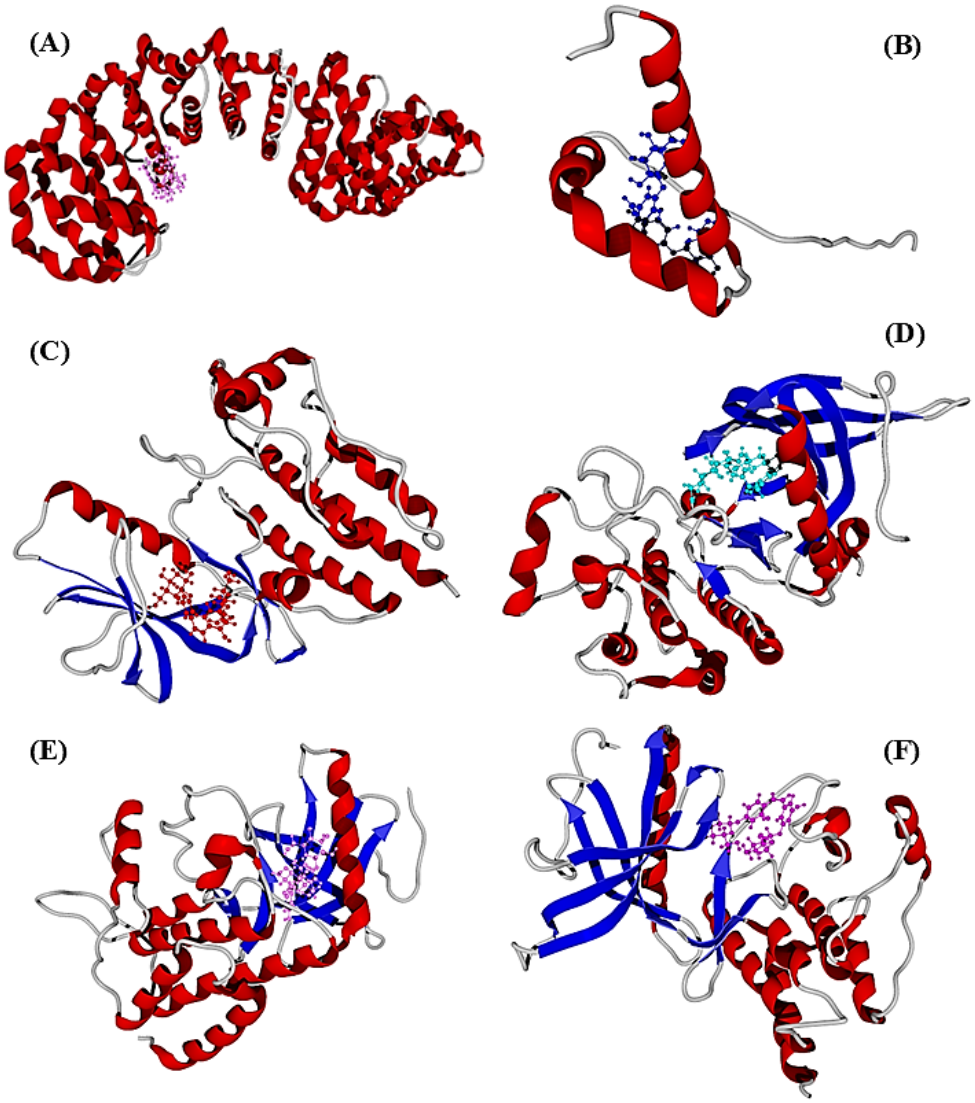

Figure 6. Docking pose of Cis-Mulberroside A with different targets (Where, (**A**): CTNNB1 Chain 1; (**B**): CTNNB1 Chain 2; (**C**): BRAF Chain 1; (**D**): EGFR Chain; (**E**): FGFR1 Chain 1; (**F**): FGFR2 Chain 2).

Table 6. Docking scores and hydrogen bond scores of the top three ligands with those of the target's positive control (approved known inhibitor).

Targets	Chain	Positive Control			Ligands		
		Name	MolDock Score	H-Bond Score	Name	MolDock Score	H-Bond Score
CTNNB1	Chain 1 (1LUJ[A])	Trametinib	−108.032	−2.904	Cis-Mulberroside A	−130.659	−15.555
					Asperuloside tetraacetate	−126.657	−8.328
					Rutin	−124.902	−16.367
	Chain 2 (1LUJ[B])	Trametinib	−130.240	0	Cis-Mulberroside A	−152.015	−20.648
					Rutin	−137.836	−11.712
					Biorobin	−133.370	−16.588
BRAF	Chain (4E26[A])	Regorafenib	−139.945	−5.165	cis-Mulberroside A	−146.515	−15.168
					Rutin	−146.206	−14.532
					Cassiaside C	−142.486	−13.824
FGFR1	Chain 1 (4V04[A])	Lenvatinib Mesylate	−150.423	−4.564	Rutin	−152.642	−15.884
					cis-Mulberroside A	−150.651	−16.732
					Asperuloside tetraacetate	−145.686	−6.768
	Chain 2 (4V04[B])	Lenvatinib Mesylate	−138.638	−5.459	cis-Mulberroside A	−162.648	−13.606
					Cassiaside C	−161.522	−19.960
					Asperuloside tetraacetate	−156.588	−2.686
EGFR	Chain (6DUK[A])	Regorafenib	−154.375	−6.178	cis-Mulberroside A	−155.333	−14.281
					Biorobin	−149.739	−17.407
					Rutin	−145.198	−9.604

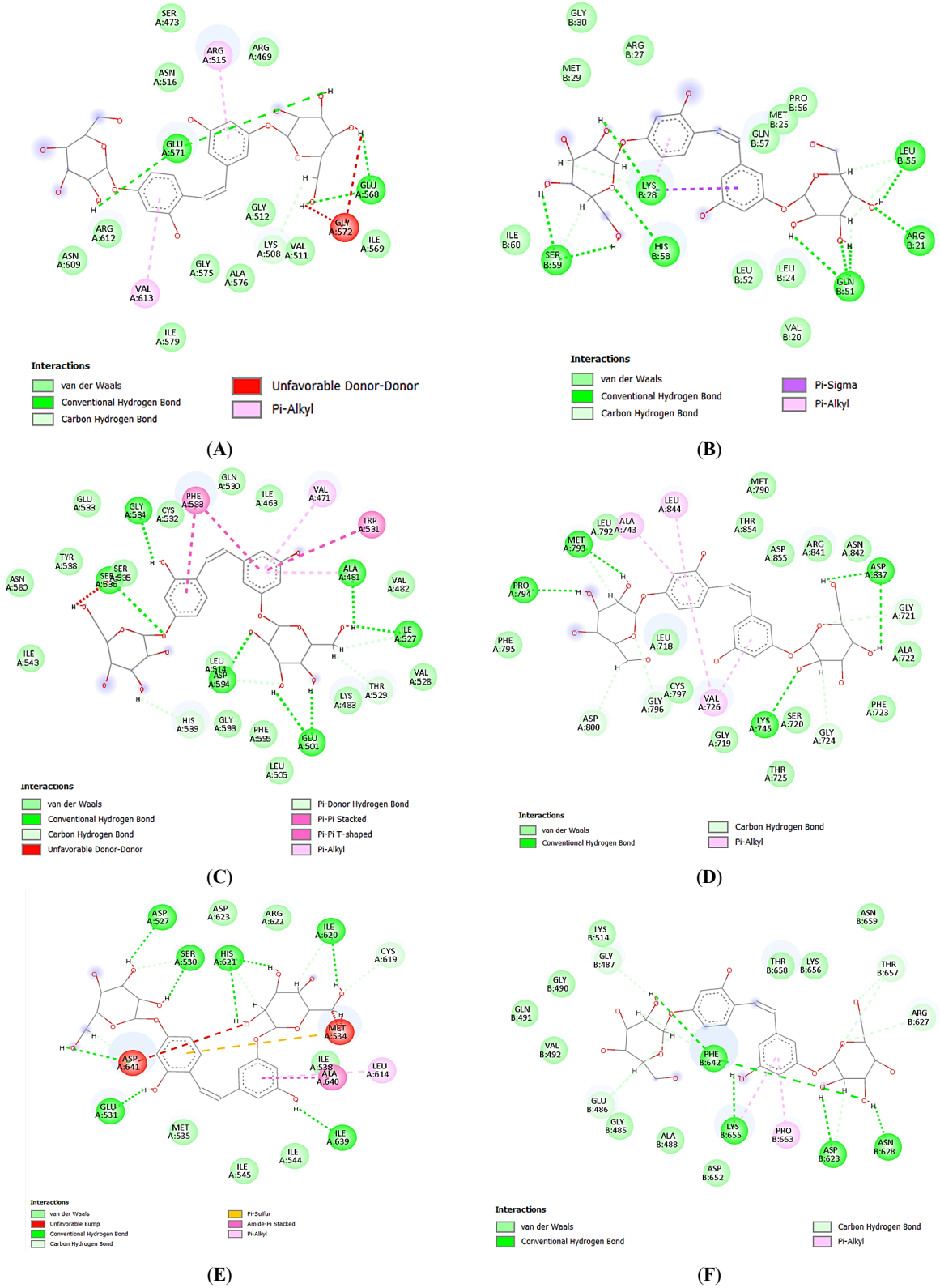

Figure 7. Docking interaction of Cis-Mulberroside A with different targets (Where, (**A**): CTNNB1 Chain 1; (**B**): CTNNB1 Chain 2; (**C**): BRAF Chain 1; (**D**): EGFR Chain; (**E**): FGFR1 Chain 1; (**F**): FGFR2 Chain 2).

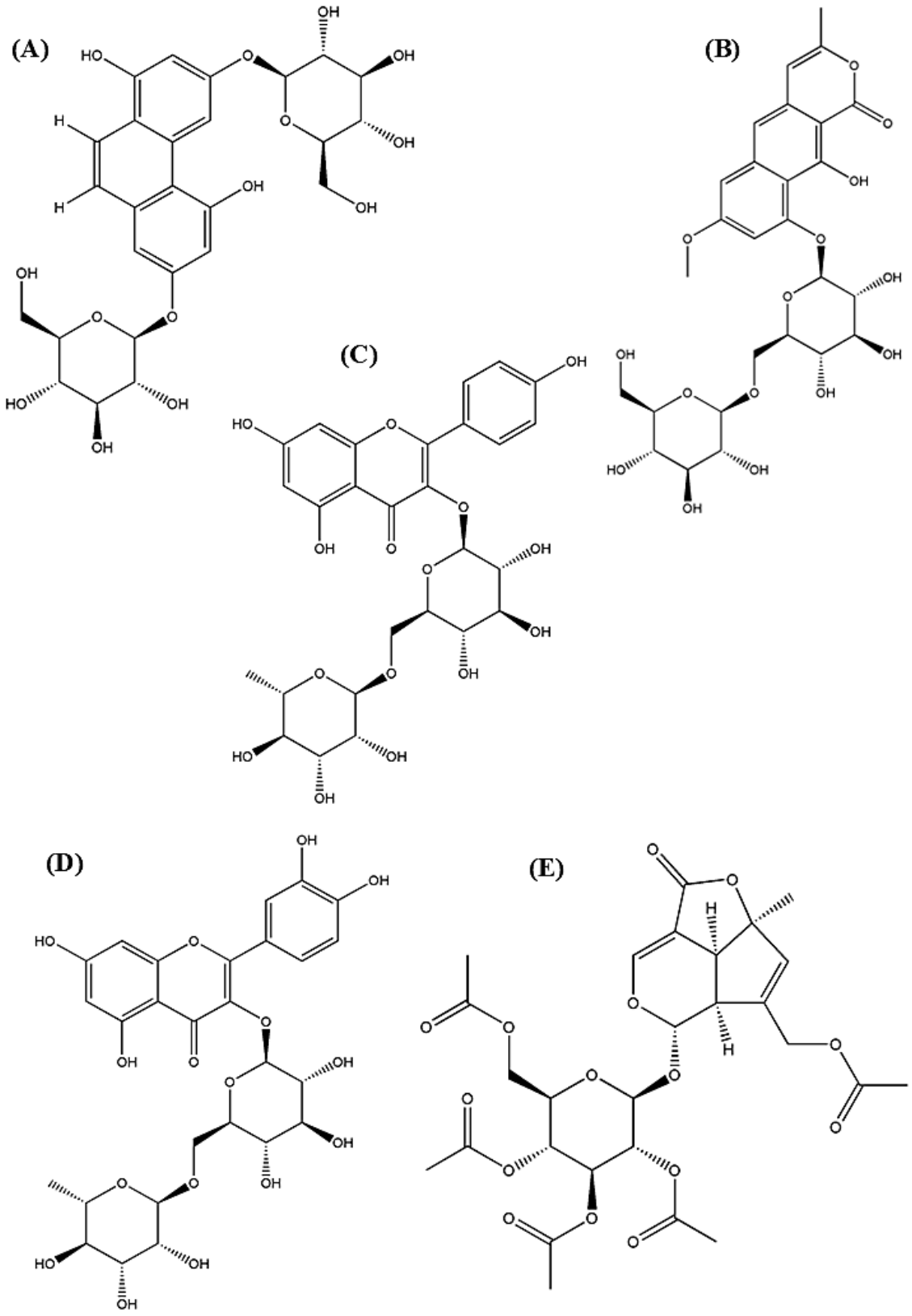

Figure 8. Chemical Structure of Compounds (**A**): Cis-Mulberroside A; (**B**): Cassiaside C; (**C**): Biorobin; (**D**): Rutin; (**E**): Asperuloside tetraacetate).

4. Discussion

Phytochemicals play vital role in neutralizing free radicals and triggering signalling responses to chemical or oxidative stress [66]. Combining these natural compounds, like isothiocyanates, quinones, carotenoids, and alkaloids, with drugs or other substances may enhance therapeutic outcomes by targeting multiple pathways while minimizing adverse effects. This approach could improve efficacy and reduce the drawbacks of conventional

treatments [67]. For centuries, herbal plant extracts have been used in traditional medicine, and many of their phytochemicals are now recognized for offering low-toxicity, natural cancer-preventive and therapeutic potential as alternatives to conventional chemotherapy [68]. These secondary metabolites have significantly contributed to treating various illnesses, not only by inhibiting, reversing, or preventing cancer progression but also by combating conditions like cancer, cardiovascular diseases, atherosclerosis, obesity, neurodegenerative disorders, diabetes, as well as inflammatory and immune-related diseases [69,70].

The primary phytochemical analysis of the extracts Methanolic extracts of the plant, *Cajanus cajan* (L.) Millsp leaves exhibited the highest antioxidant activity. These findings highlight its strong antioxidant affinity, supported by both qualitative and quantitative evaluations. The plant extracts demonstrate the appearance of antioxidant enzymes such as SOD and CAT, which are important in managing and counteracting the detrimental impacts of free radicals or reactive oxygen species (ROS) produced during metabolic activities. Many plants exhibit considerable reactive oxygen species (ROS) scavenging (antioxidant) ability, which is associated with their ability to inhibit cancer cell proliferation (cytotoxicity). It provides an abundance of wellness benefits, including antifungal [71], antimicrobial [72,73], anti-inflammatory [74,75], cholesterol-lowering [76], anti-diabetic [77], anti-cancer [78], neuroprotective [79], antioxidant [75,80], liver-protective [81] and glycemic-regulating effects [77,82], among others. The extracts of *Cajanus cajan* demonstrated promising activity against eight microbial strains, including *Staphylococcus epidermidis*, *Bacillus subtilis*, *Proteus vulgaris*, *Escherichia coli*, *Aspergillus niger*, and *Candida albicans* [72,83]. The methanol extract of *C. cajan* leaves demonstrated significant antimicrobial activity, effectively inhibiting the growth of *Escherichia coli* and *Candida albicans* [73]. Through bioassay-guided fractionation of *Cajanus cajan* leaf extracts using chloroform, researchers identified new natural coumarins, including cajanuslactone, along with two phytoalexins: pinostrobin and cajaninstilbene acid. Notably, cajanuslactone has shown a strong antibacterial effect, especially against *Staphylococcus aureus* [84]. An HPLC-FRAP analysis revealed the presence of bioactive compounds of bark extract of *C. cajan* stem, each showing potential antioxidant activity [85]. *Cajanus cajan* has also been employed for its neuroprotective properties. Its stilbenoids can induce apoptotic neuronal death following Aβ25–35 injection in mice, leading to increased activity of choline acetyltransferase (ChAT) and superoxide dismutase (SOD) in the cortex and hippocampus [74,79]. The roots of *Cajanus cajan* contain cajanol, an isoflavanone recognized as a significant phytoalexin. Studies have investigated its anticancer effects specifically against MCF-7 human breast cancer cells [78,86–88].

The methanolic extracts of the plant *Cajanus cajan* (L.) Millsp with the highest potential were subjected to metabolite profiling through LC-MS, based on biochemical analysis. To determine possible targets for drugs for Hepatocellular carcinoma (HCC), a gene networking strategy has been adopted. Analyzing gene networks aids in uncovering potential genes that might be used as viable drug targets within large-scale networks [89–91]. The application of protein-ligand molecular docking is fundamental in drug discovery, as it helps to assess the therapeutic properties and mode of action of new compounds [92–94]. Gene network analysis has revealed CTNNB1 as crucial gene linked to hepatocellular carcinoma (HCC). Alongside this significant gene, additional drug targets associated with HCC, drawn from the existing literature, have been incorporated. These include BRAF, EGFR and FGFR1. This computational analysis indicates that all of the selected ligands are capable of interacting with the eight target proteins in a manner comparable to their known inhibitors or drugs. The more negative the score, the stronger the binding affinity. Among all the cis-mulberroside A exhibited superior binding affinity compared to the positive controls for all targets. The cis-mulberroside A identified from *Cajanus cajan* (L.) Millsp has been shown, through molecular docking, to have the potential binding affinity against the targets of HCC. Present findings indicate that cis-mulberroside A exhibits significant inhibitory potential due to its higher binding affinity, suggesting it as a strong candidate for inhibiting HCC targets. The study disclosed that cis-mulberroside A binding energy is notably lower than that of the positive controls, indicating superior binding affinity. Additionally, hydrogen bonding is essential for ligand-protein interactions, and cis-mulberroside A demonstrated a greater number of hydrogen bonds with target proteins than the positive controls. Based on docking scores and hydrogen bond analysis, the in-silico studies support cis-mulberroside A as a promising inhibitory potential against various HCC targets.

The compound, cis-mulberroside A, also known as mulberroside D, is reported to have potential in treating various cancers by against key signaling pathways. It also has diverse therapeutic effects in other diseases, including antioxidant, anti-inflammatory and anti-diabetic properties [95,96]. Extracts containing cis-mulberroside A and other phenolic compounds can inhibit the growth of HepG2 hepatoma cells. This effect involves causing cell cycle arrest (specifically in the G2/M phase) and inducing apoptosis (programmed cell death). It can block signaling pathways (such as NF-κB, STAT3, and Akt/mTOR) that are activated by pro-inflammatory cytokines like TNF-α and IL-6, which are released by adipocytes and promote hepatoma cell proliferation. cis-mulberroside A protects liver cells from damage induced by toxins like alcohol and CCl4 (carbon tetrachloride) by enhancing

antioxidant enzyme activity, reducing lipid peroxidation, and mitigating inflammation [97–101]. The phytochemicals interact with key molecular markers involved in cancer progression, such as down-regulating cyclin D1 and activating ATF3 expression, which contribute to cell growth inhibition and apoptosis in cancer cells. Cis-mulberroside A phytochemicals are associated with a wide range of other health benefits and therapeutic potentials. cis-mulberroside A has potent anti-inflammatory properties, reducing the production of inflammatory mediators like nitric oxide (NO), TNF-α, IL-6, and IL-1β by inhibiting the activation of pathways like NF-κB and MAPK [102]. This makes it a potential therapeutic candidate for various inflammatory conditions, including osteoarthritis. cis-mulberroside A and its aglycone, oxyresveratrol, act as strong antioxidants, scavenging free radicals and reducing oxidative stress that is implicated in chronic diseases and ageing. Mulberry extracts and mulberrosides help regulate blood glucose levels and improve insulin sensitivity. These compounds exhibit neuroprotective effects, such as protecting against cerebral ischemia and potentially offering therapeutic effects in neurodegenerative disorders like Parkinson's disease, cis-mulberroside A helps mitigate cellular senescence, enhances resistance to oxidative stress, and has been used in cosmetics for its skin-whitening effects by inhibiting melanin synthesis. cis-mulberroside A can inhibit the migration of vascular smooth muscle cells and help reduce the risk of atherosclerosis [96,103,104]. The results indicate that *Cajanus cajan* (L.) Millsp phytochemicals capable of modulating key cancer-related pathways. Among the screened compounds, Cis-Mulberroside A (Mulberroside D) demonstrated the strongest binding toward CTNNB1, BRAF, FGFR, and EGFR, surpassing their respective positive controls. This highlights Mulberroside D as a promising inhibitor of major dysregulated signaling targets in hepatocellular carcinoma (HCC).

5. Conclusions

The study focuses on the anti-cancerous effect of *Cajanus cajan* (L.) Millsp phytochemical and it provides initial evidence that *Cajanus cajan* (L.) Millsp, contains bioactive molecules capable of influencing pathways relevant to cancers and may serve as valuable source of anticancer phytoconstituents. The identified compounds from metabolite profiling of the plant were evaluated using Molecular Docking approaches, where Cis-Mulberroside A, Asperuloside tetraacetate, Rutin, Biorobin and Cassiaside C showed better binding efficiency with the selected targets compared with the positive controls of respective targets. Among these, Cis-Mulberroside A (also referred to as Mulberroside D), a stilbenoid glycoside, exhibited the highest binding affinity with CTNNB1, BRAF, FGFR and EGFR. These results of molecular docking scores and hydrogen bonding analysis of Cis-Mulberroside A, with the selected targets and positive control revealed that Cis-Mulberroside A holds significant inhibitory potential against critical targets in hepatocellular carcinoma (HCC), particularly CTNNB1, BRAF, FGFR and EGFR, which are commonly associated with HCC. These findings indicate that Cis-Mulberroside A has a lower binding energy than the positive control, indicating higher affinity, and forms significant hydrogen bonds with the target protein, which emphasizes the significance of hydrogen bonding in ligand-protein interactions. These findings highlight its potential as a potent candidate for anti-cancer lead development against HCC targets. Further investigations like *in-vitro* or *in-vivo* and clinical studies will need for the validation of its efficacy in development and employing as a future lead for liver cancer treatment.

Supplementary Materials: The following supporting information can be downloaded at: https://media.sciltp.com/articles/others/2601261008235749/JMNP-25120101-Supplementary-Materials.zip.

Author Contributions: S.K.: Data curation, data analysis, writing—original draft & preparation; P.N., T.A., S.D.S. and M.A.L.: Writing—reviewing and editing; S.K., D.N., and A.D.T.: Writing—original draft, methodology, software, Formal Analysis, Writing—reviewing and editing, Conceptualization, visualization, methodology, investigation, supervision, software, writing—reviewing and final editing. All authors have read and agreed to the published version of the manuscript.

Funding: This research received no external funding.

Institutional Review Board Statement: Not applicable.

Informed Consent Statement: Not applicable.

Data Availability Statement: Data that support the findings of this study are available in the supplementary material of this article.

Acknowledgements: The authors are grateful to the Bioinformatics and Computational Biology Centre at Assam University, Silchar, for software support through the DBT-Bioinformatics Infrastructure Facility, and e-journal access facility through the DBT e-Library Consortium (DeLCON) and also thankful to Shuvasish Choudhury of the Department of Life Science and Bioinformatics, Assam University, for supporting with Molegro Virtual Docker 6.0 software.

Conflicts of Interest: The authors declare no conflict of interest.

Use of AI and AI-Assisted Technologies: No AI tools were utilized for this paper.

Abbreviations

Ac	Absorbance of the control
ADAM17	A Disintegrin and Metalloproteinase 17
Akt/mTOR	Protein kinase B/Mammalian target of rapamycin
$AlCl_3$	Aluminium Chloride
AR (Amphiregulin)	Amphiregulin
At	Absorbance of the test sample
AUSCH	Assam University Silchar Central Herbarium
AXIN1	Axis inhibition protein 1
BRAF	B-Raf Proto-Oncogene, Serine/Threonine Kinase
BSA	Bovine serum albumin
BTC (Betacellulin)	Betacellulin
CASP8	Caspase 8
CAT	Catalase
CCl_4	Carbon tetrachloride
ChAT	Choline acetyltransferase
Conc. HCl	Concentrated hydrochloric acid
CTNNB1	Catenin beta 1
DAVID	Database for Annotation, Visualization and Integrated Discovery
DPPH	2,2-diphenyl-1-picrylhydrazyl
DTC	Differentiated Thyroid Carcinoma
EGF	Epidermal Growth Factor
EGFR	Epidermal Growth Factor Receptor
ERK	Extracellular Signal-Regulated Kinase
ESI-	Electron spray Ionization
FA	Formic acid
FGFR	Fibroblast Growth Factor Receptor
FRAP	Ferric Reducing Antioxidant Power
GAE/mg	Gallic acid equivalents per milligram
GLOBOCAN	Global Cancer Observatory
H_2O_2	Hydrogen peroxide
HB-EGF	Heparin-Binding Epidermal Growth Factor
HCC	Hepatocellular carcinoma
HCl	Hydrochloric acid
$HgCl_2$	Mercuric chloride
HPLC	High Performance Liquid Chromatography
HRLC	High-Resolution Liquid Chromatography
IC_{50}	Half maximal inhibitory concentration
IL-6	Interleukin 6
KEGG	Kyoto Encyclopedia of Genes and Genomes
KI	Potassium Iodide
LCMS	Liquid Chromatography Mass Spectrometry
MAPK	Mitogen-activated protein kinase
MASLD	Metabolic dysfunction-associated steatotic liver disease
MCODE	Molecular Complex Detection
MCF-7	Michigan Cancer Foundation-7
MEK	Mitogen-Activated Protein Kinase Kinase
MVD	Molegro Virtual Docker
Na_2CO_3	Sodium carbonate
NBT	Nitroblue tetrazolium
NCBI	National Center for Biotechnology Information.
NF-κB	Nuclear factor kappa-light-chain-enhancer of activated B cells
NO	Nitric oxide
OMIM	Online Mendelian Inheritance in Man
PDB	Protein Data Bank
PMSF	Phenylmethanesulfonyl fluoride
PPI	Protein–protein interaction
PVP	Polyvinyl pyrrolidone
QE/mg	Quercetin equivalents per milligram
RCC	Renal Cell Carcinoma
RAF	Rapidly Accelerated Fibrosarcoma
RAS	Rat Sarcoma
ROS	Reactive Oxygen Species
RRHT	Rapid Resolution High Throughput
SOD	Superoxide dismutase
STAT3	Signal transducer and activator of transcription 3
TCGA	Cancer Genome Atlas Program
TFC	Total Flavonoid Content
TGF-α	Transforming Growth Factor-alpha

TKI	Tyrosine Kinase Inhibitor
TP53	Tumor protein p53
TPC	Total Phenolic Content
VEGFR	Vascular Endothelial Growth Factor Receptor
WHO	World Health Organization
Wnt	Wingless-related integration

References

1. Islam, M.R.; Rauf, A.; Alash, S.; et al. A comprehensive review of phytoconstituents in liver cancer prevention and treatment: Targeting insights into molecular signaling pathways. *Med. Oncol.* **2024**, *41*, 134.
2. Li, S.; Yin, S.; Ding, H.; et al. Polyphenols as potential metabolism mechanisms regulators in liver protection and liver cancer prevention. *Cell Proliferat.* **2023**, *56*, e13346.
3. Niu, C.; Zhang, J.; Okolo, P.I. Liver cancer wars: Plant-derived polyphenols strike back. *Med. Oncol.* **2024**, *41*, 106.
4. Giri, S.; Singh, A. Epidemiology of Hepatocellular Carcinoma in India–An Updated Review for 2024. *J. Clin. Exp. Hepatol.* **2024**, *14*, 101447.
5. Yang, F.; Sun, D.; Xia, C.; et al. Global trajectories of liver cancer burden from 1990 to 2019 and projection to 2035. *Chin. Med. J.* **2023**, *136*, 1413–1421.
6. Mak, L.-Y.; Liu, K.; Chirapongsathorn, S.; et al. Liver diseases and hepatocellular carcinoma in the Asia-Pacific region: Burden, trends, challenges and future directions. *Nat. Rev. Gastro. Hepat.* **2024**, *21*, 387–404.
7. Urquijo-Ponce, J.J.; Alventosa-Mateu, C.; Latorre-Sánchez, M.; et al. Present and future of new systemic therapies for early and intermediate stages of hepatocellular carcinoma. *World J. Gastroenterol.* **2024**, *30*, 2512–2525.
8. Yang, J.D.; Hainaut, P.; Gores, G.J.; et al. A global view of hepatocellular carcinoma: Trends, risk, prevention and management. *Nat. Rev. Gastro. Hepat.* **2019**, *16*, 589–604.
9. Rumgay, H.; Arnold, M.; Ferlay, J.; et al. Global burden of primary liver cancer in 2020 and predictions to 2040. *J. Hepatol.* **2022**, *77*, 1598–1606.
10. Bray, F.; Laversanne, M.; Sung, H.; et al. Global cancer statistics 2022: GLOBOCAN estimates of incidence and mortality worldwide for 36 cancers in 185 countries. *CA Cancer J. Clin.* **2024**, *74*, 229–263.
11. Sun, J.; Luo, Q.; Liu, L.; et al. Low-level shear stress promotes migration of liver cancer stem cells via the FAK-ERK1/2 signalling pathway. *Cancer Lett.* **2018**, *427*, 1–8.
12. Abou-El-Enein, M.; Grainger, D.W.; Kili, S. Registry contributions to strengthen cell and gene therapeutic evidence. *Mol. Ther.* **2018**, *26*, 1172–1176.
13. Ma, Y.-S.; Liu, J.-B.; Wu, T.-M.; et al. New therapeutic options for advanced hepatocellular carcinoma. *Cancer Control* **2020**, *27*, 1073274820945975.
14. Liu, W.; Cui, X.; Zhong, Y.; et al. Phenolic metabolites as therapeutic in inflammation and neoplasms: Molecular pathways explaining their efficacy. *Pharmacol. Res.* **2023**, *193*, 106812.
15. Mathew, S.; Faheem, M.; Suhail, M.; et al. Updates on traditional medicinal plants for hepatocellular carcinoma. *Pharmacogn. J.* **2016**, *8*, 203–214.
16. Monsuez, J.-J.; Charniot, J.-C.; Vignat, N.; et al. Cardiac side-effects of cancer chemotherapy. *Int. J. Cardiol.* **2010**, *144*, 3–15.
17. Raoul, J.-L.; Kudo, M.; Finn, R.S.; et al. Systemic therapy for intermediate and advanced hepatocellular carcinoma: Sorafenib and beyond. *Cancer Treat. Rev.* **2018**, *68*, 16–24.
18. Lee, J.K.; Abou-Alfa, G.K. An update on clinical trials in the treatment of advanced hepatocellular carcinoma. *J. Clin. Gastroenterol.* **2013**, *47*, S16–S19**.**
19. Bruix, J.; Tak, W.-Y.; Gasbarrini, A.; et al. Regorafenib as second-line therapy for intermediate or advanced hepatocellular carcinoma: Multicentre, open-label, phase II safety study. *Eur. J. Cancer* **2013**, *49*, 3412–3419.
20. Chuma, M.; Terashita, K.; Sakamoto, N. New molecularly targeted therapies against advanced hepatocellular carcinoma: From molecular pathogenesis to clinical trials and future directions. *Hepatol. Res.* **2015**, *45*, E1–E11.
21. Kudo, M.; Finn, R.S.; Qin, S.; et al. Lenvatinib versus sorafenib in first-line treatment of patients with unresectable hepatocellular carcinoma: A randomised phase 3 non-inferiority trial. *Lancet* **2018**, *391*, 1163–1173.
22. Cheng, A.-L.; Finn, R.S.; Qin, S.; et al. Phase III trial of lenvatinib (LEN) vs sorafenib (SOR) in first-line treatment of patients (pts) with unresectable hepatocellular carcinoma (uHCC). *J. Clin. Oncol.* **2017**, *35*, 4001–4015.
23. Rimassa, L.; Danesi, R.; Pressiani, T.; et al. Management of adverse events associated with tyrosine kinase inhibitors: Improving outcomes for patients with hepatocellular carcinoma. *Cancer Treat. Rev.* **2019**, *77*, 20–28.
24. García, E.R.; Gutierrez, E.A.; Melo, F.C.S.A.d.; et al. Flavonoids effects on hepatocellular carcinoma in murine models: A systematic review. *Evid. Based Compl. Alt.* **2018**, *2018*, 6328970.
25. Dantzer, C.; Dif, L.; Vache, J.; et al. Specific features of ß-catenin-mutated hepatocellular carcinomas. *Br. J. Cancer* **2024**, *131*, 1871–1880.
26. Xu, C.; Xu, Z.; Zhang, Y.; et al. β-Catenin signaling in hepatocellular carcinoma. *J. Clin. Invest.* **2022**, *132*, e154515.

27. Qiao, Q.; Zhang, J.; Wang, W.; et al. Over expression of transforming growth factor-alpha and epidermal growth factor receptor in human hepatic cirrhosis tissues. *Hepatogastroenterology* **2008**, *55*, 169–172.
28. Harada, K.I.; Shiota, G.; Kawasaki, H. Transforming growth factor-α and epidermal growth factor receptor in chronic liver disease and hepatocellular carcinoma. *Liver* **1999**, *19*, 318–325.
29. Funakoshi-Tago, M.; Okamoto, K.; Izumi, R.; et al. Anti-inflammatory activity of flavonoids in Nepalese propolis is attributed to inhibition of the IL-33 signaling pathway. *Int. Immunopharmacol.* **2015**, *25*, 189–198.
30. Bhatt, N.; Deshpande, M. A critical review of Indian medicinal plants for hepatocellular carcinoma. *Int. J. Ayurvedic Herb Med.* **2022**, *12*, 4150–4186.
31. Rawat, D.; Shrivastava, S.; Naik, R.A.; et al. An overview of natural plant products in the treatment of hepatocellular carcinoma. *Anti Cancer Agents Med. Chem.* **2018**, *18*, 1838–1859.
32. Mandlik, D.S.; Mandlik, S.K. Herbal and natural dietary products: Upcoming therapeutic approach for prevention and treatment of hepatocellular carcinoma. *Nutr. Cancer* **2021**, *73*, 2130–2154.
33. Adekilekun, H.A.; Oyewusi, H.A.; Odoma, S.; et al. An Overview of Traditional Medicinal Plants Used in Treating Hepatocellular Carcinoma (HCC) with Emphasis on Mechanisms of Action: Traditional Medicinal Treatment of Hepatocellular Carcinoma (HCC). *J. Trop. Life Sci.* **2024**, *14*, 405–428.
34. Nasreen, S.; Safeer, S.; Dar, K.K.; et al. Etiology of hepatocellular carcinoma and treatment through medicinal plants: A comprehensive review. *Orient. Pharm. Exp. Med.* **2018**, *18*, 187–197.
35. Saeed, R.A.; Maqsood, M.; Saeed, R.A.; et al. Plant-based foods and hepatocellular carcinoma: A review on mechanistic understanding. *Crit. Rev. Food Sci.* **2023**, *63*, 11750–11783.
36. Yang, S.-E.; Vo, T.-L.T.; Chen, C.-L.; et al. Nutritional composition, bioactive compounds and functional evaluation of various parts of *Cajanus cajan* (L.) Millsp. *Agriculture* **2020**, *10*, 558.
37. Mathew, D.; Manila, T.; Divyasree, P.; et al. Therapeutic molecules for multiple human diseases identified from pigeon pea (*Cajanus cajan* L. Millsp.) through GC–MS and molecular docking. *Food Sci. Hum. Well.* **2017**, *6*, 202–216.
38. Abubakar, A.R.; Haque, M. Preparation of medicinal plants: Basic extraction and fractionation procedures for experimental purposes. *J. Pharm. Bioallied Sci.* **2020**, *12*, 1–10.
39. Bakir Çilesizoğlu, N.; Yalçin, E.; Çavuşoğlu, K.; et al. Qualitative and quantitative phytochemical screening of *Nerium oleander* L. extracts associated with toxicity profile. *Sci. Rep.* **2022**, *12*, 21421.
40. Evans, W. *Trease and Evans Pharmacognosy*, 15th ed.; Saunders Publishers: Philadelphia, PA, USA, 2002.
41. Shaikh, J.R.; Patil, M. Qualitative tests for preliminary phytochemical screening: An overview. *Int. J. Chem. Stud.* **2020**, *8*, 603–608.
42. Siddiqui, A.A.; Ali, M. *Practical Pharmaceutical Chemistry*; CBS Publishers & Distributors: Patparganj, Delhi, 1997.
43. Sofowara, A. *Medicinal Plants and Traditional Medicine in Africa Spectrum Books LTD*; Spectrum Books Ltd.: Ibadan, Nigeria, 1993.
44. Sankhalkar, S.; Vernekar, V. Quantitative and qualitative analysis of phenolic and flavonoid content in *Moringa oleifera* Lam and *Ocimum tenuiflorum* L. *Pharmacogn. Res.* **2016**, *8*, 16–22.
45. Sati, S.; Kumar, P. Assessment of Himalayan juniper, *Juniperus squamata* buch–ham ex d. don for phytochemical screening and antimicrobial potential against some infection causing pathogens. *World J. Pharmaceut. Res.* **2015**, *4*, 998–1011.
46. Archana, P.; Samatha, T.; Mahitha, B.; et al. Preliminary phytochemical screening from leaf and seed extracts of *Senna alata* L. Roxb-an ethnomedicinalplant. *Int. J. Pharm. Sci. Res.* **2012**, *3*, 82–89.
47. Auwal, M.S.; Saka, S.; Mairiga, I.A.; et al. Preliminary phytochemical and elemental analysis of aqueous and fractionated pod extracts of *Acacia nilotica* (Thorn mimosa). *Vet. Res. Forum* **2014**, *5*, 95–100.
48. Singleton, V.L.; Orthofer, R.; Lamuela-Raventós, R.M. [14] Analysis of total phenols and other oxidation substrates and antioxidants by means of folin-ciocalteu reagent. *Method. Enzymol.* **1999**, *299*, 152–178.
49. Lamuela-Raventós, R.M. Folin–Ciocalteu Method for the Measurement of Total Phenolic Content and Antioxidant Capacity. In *Measurement of Antioxidant Activity & Capacity;* John Wiley & Sons: Hoboken, NJ, USA, 2018; pp. 107–115.
50. Arvouet-Grand, A.; Vennat, B.; Pourrat, A.; et al. Standardization of propolis extract and identification of principal constituents. *J. Pharm. Belg.* **1994**, *49*, 462–468.
51. Shraim, A.M.; Ahmed, T.A.; Rahman, M.M.; et al. Determination of total flavonoid content by aluminum chloride assay: A critical evaluation. *Lwt* **2021**, *150*, 111932.
52. Kumarasamy, Y.; Byres, M.; Cox, P.J.; et al. Screening seeds of some Scottish plants for free radical scavenging activity. *Phytother. Res.* **2007**, *21*, 615–621.
53. Gulcin, İ.; Alwasel, S.H. DPPH radical scavenging assay. *Processes* **2023**, *11*, 2248.
54. Almulaiky, Y.Q.; Aldhahri, M.; Al-abbasi, F.A.; et al. *In vitro* assessment of antioxidant enzymes, phenolic contents and antioxidant capacity of the *verdolaga* (*Portulacaceae*). *Int. J. Nutr.* **2020**, *4*, 36–47.
55. Mehraj, S.S.; Kamili, A.N.; Nazir, R.; et al. Comparative evaluation of extraction methods for total proteins from *Crocus sativus* L. (*Saffron*). *Saudi J. Biol. Sci.* **2018**, *25*, 1603–1608.

56. Aebi, H. [13] Catalase *in vitro*. *Method. Enzymol.* **1984**, *105*, 121–126.
57. Tekin, S.; Seven, E. Assessment of serum catalase, reduced glutathione, and superoxide dismutase activities and malondialdehyde levels in keratoconus patients. *Eye* **2022**, *36*, 2062–2066.
58. Beyer, W.F., Jr.; Fridovich, I. Assaying for superoxide dismutase activity: Some large consequences of minor changes in conditions. *Anal. Biochem.* **1987**, *161*, 559–566.
59. Chen, X.; Li, D.; Guo, J.; et al. Identification and analysis of the superoxide dismutase (SOD) gene family and potential roles in high-temperature stress response of herbaceous peony (*Paeonia lactiflora* pall.). *Antioxidants* **2024**, *13*, 1128.
60. Szklarczyk, D.; Kirsch, R.; Koutrouli, M.; et al. The STRING database in 2023: Protein–protein association networks and functional enrichment analyses for any sequenced genome of interest. *Nucleic Acids Res.* **2023**, *51*, D638–D646**.**
61. Rivera, C.G.; Vakil, R.; Bader, J.S. NeMo: Network module identification in Cytoscape. *BMC Bioinformatics* **2010**, *11*, S61.
62. Su, G.; Morris, J.H.; Demchak, B.; et al. Biological network exploration with Cytoscape 3. *Curr. Protoc. Bioinform.* **2014**, *47*, 8.13.1–8.13.24.
63. Sherman, B.T.; Hao, M.; Qiu, J.; et al. DAVID: A web server for functional enrichment analysis and functional annotation of gene lists (2021 update). *Nucleic Acids Res.* **2022**, *50*, W216–W221**.**
64. Bitencourt-Ferreira, G.; de Azevedo, W.F. Molegro Virtual Docker for Docking. In *Docking Screens for Drug Discovery*; Springer: New York, NY, USA, 2019; pp. 149**–**167.
65. Dere, D.; Pehlivan, S.N.; da Silva, A.D.; et al. Hands-On Docking with Molegro Virtual Docker. *In Docking Screens for Drug Discovery*; Springer: New York, NY, USA, 2025; pp. 125**–**138.
66. Rivera-Pérez, J.; Martínez-Rosas, M.; Conde-Castañón, C.A.; et al. Epigallocatechin 3-gallate has a neuroprotective effect in retinas of rabbits with ischemia/reperfusion through the activation of Nrf2/HO-1. *Int. J. Mol. Sci.* **2020**, *21*, 3716.
67. Deng, X.; Yang, Z.; Han, M.; et al. Comprehensive Insights into the Combinatorial Uses of Selected Phytochemicals in Colorectal Cancer Prevention and Treatment: Isothiocyanates, Quinones, Carotenoids, and Alkaloids. *Phytother. Res.* **2024**, *38*, 2884–2907.
68. Nadia, M.; Maryam, M. Use of Medicinal Plants for The Treatment of Cancer in Different Parts of The World: An Overview. *Adv. J. Chem. A* **2024**, *7*, 189–199.
69. Gezici, S.; Şekeroğlu, N. Current perspectives in the application of medicinal plants against cancer: Novel therapeutic agents. *Anti Cancer Agents Med. Chem.* **2019**, *19*, 101–111.
70. Teiten, M.-H.; Gaascht, F.; Dicato, M.; et al. Anticancer bioactivity of compounds from medicinal plants used in European medieval traditions. *Biochem. Pharmacol.* **2013**, *86*, 1239–1247.
71. Brito, S.A.; Rodrigues, F.F.; Campos, A.R.; et al. Evaluation of the antifungal activity and modulation between *Cajanus cajan* (L.) Millsp. leaves and roots ethanolic extracts and conventional antifungals. *Pharmacogn. Mag.* **2012**, *8*, 103.
72. Zu, Y.-G.; Liu, X.-L.; Fu, Y.-J.; et al. Chemical composition of the SFE-CO2 extracts from *Cajanus cajan* (L.) Huth and their antimicrobial activity *in vitro* and *in vivo*. *Phytomedicine* **2010**, *17*, 1095–1101.
73. Dinore, J.M.; Farooqui, M. GC-MS and LC-MS: An integrated approach towards the phytochemical evaluation of methanolic extract of Pigeon Pea [*Cajanus cajan* (L.) Millsp] leaves. *Nat. Prod. Res.* **2022**, *36*, 2177–2181.
74. Huang, M.-Y.; Lin, J.; Lu, K.; et al. Anti-inflammatory effects of cajaninstilbene acid and its derivatives. *J. Agric. Food Chem.* **2016**, *64*, 2893–2900.
75. Vo, T.-L.T.; Yang, N.-C.; Yang, S.-E.; et al. Effects of *Cajanus cajan* (L.) millsp. roots extracts on the antioxidant and anti-inflammatory activities. *J. Physiol. Invest.* **2020**, *63*, 137–148.
76. Nicholson, R.A.; David, L.S.; Le Pan, R.; et al. Pinostrobin from *Cajanus cajan* (L.) Millsp. inhibits sodium channel-activated depolarization of mouse brain synaptoneurosomes. *Fitoterapia* **2010**, *81*, 826–829.
77. Nahar, L.; Nasrin, F.; Zahan, R.; et al. Comparative study of antidiabetic activity of *Cajanus cajan* and *Tamarindus indica* in alloxan-induced diabetic mice with a reference to *in vitro* antioxidant activity. *Pharmacogn. Res.* **2014**, *6*, 180–187.
78. Luo, M.; Liu, X.; Zu, Y.; et al. Cajanol, a novel anticancer agent from Pigeonpea [*Cajanus cajan* (L.) Millsp.] roots, induces apoptosis in human breast cancer cells through a ROS-mediated mitochondrial pathway. *Chem.-Biol. Interact.* **2010**, *188*, 151–160.
79. Kim, Y.C. Neuroprotective phenolics in medicinal plants. *Arch. Pharm. Res.* **2010**, *33*, 1611–1632.
80. Aggarwal, A.; Nautiyal, U.; Negi, D. Characterization and evaluation of antioxidant activity of *Cajanus cajan* and *Pisum sativum*. *Int. J. Recent Adv. Sci. Technol.* **2015**, *2*, 21–26.
81. Wang, X.-Q.; Wei, W.; Zhao, C.-J.; et al. Negative-pressure cavitation coupled with aqueous two-phase extraction and enrichment of flavonoids and stilbenes from the pigeon pea leaves and the evaluation of antioxidant activities. *Sep. Purif. Technol.* **2015**, *156*, 116–123.
82. Duker-Eshun, G.; Jaroszewski, J.W.; Asomaning, W.A.; et al. Antiplasmodial constituents of *Cajanus cajan*. *Phytother. Res.* **2004**, *18*, 128–130.
83. Abo-Zeid, M.A.; Abdel-Samie, N.S.; Farghaly, A.A.; et al. Flavonoid fraction of *Cajanus cajan* prohibited the mutagenic properties of cyclophosphamide in mice *in vivo*. *Mutat. Res. Gen. Tox. En.* **2018**, *826*, 1–5.

84. Orni, P.R.; Ahmed, S.Z.; Monefa, M.; et al. Pharmacological and phytochemical properties of *Cajanus cajan* (L.) Huth. (Fabaceae): A review. *Int. J. Pharm. Sci. Res.* **2018**, *9*, 886–894.
85. Sinan, K.I.; Mahomoodally, M.F.; Eyupoglu, O.E.; et al. HPLC-FRAP methodology and biological activities of different stem bark extracts of *Cajanus cajan* (L.) Millsp. *J. Pharm. Biomed. Anal.* **2021**, *192*, 113678.
86. Ashidi, J.; Houghton, P.; Hylands, P.; et al. Ethnobotanical survey and cytotoxicity testing of plants of South-western Nigeria used to treat cancer, with isolation of cytotoxic constituents from *Cajanus cajan* Millsp. leaves. *J. Ethnopharmacol.* **2010**, *128*, 501–512.
87. Lim, T.; Lim, T. *Cajanus cajan*. In *Edible Medicinal and Non-Medicinal Plants*; Springer: Dordrecht, Netherlands, 2012; Volume 2, pp. 549–568**.**
88. Hassan, E.M.; Matloub, A.A.; Aboutabl, M.E.; et al. Assessment of anti-inflammatory, antinociceptive, immunomodulatory, and antioxidant activities of *Cajanus cajan* L. seeds cultivated in Egypt and its phytochemical composition. *Pharm. Biol.* **2016**, *54*, 1380–1391.
89. Zhou, L.; Du, Y.; Kong, L.; et al. Identification of molecular target genes and key pathways in hepatocellular carcinoma by bioinformatics analysis. *OncoTargets Ther.* **2018**, *11*, 1861–1869.
90. Tong, Z.; Zhou, Y.; Wang, J. Identifying potential drug targets in hepatocellular carcinoma based on network analysis and one-class support vector machine. *Sci. Rep.* **2019**, *9*, 10442.
91. Wang, J.; Peng, R.; Zhang, Z.; et al. [Retracted] Identification and Validation of Key Genes in Hepatocellular Carcinoma by Bioinformatics Analysis. *BioMed Res. Int.* **2021**, *2021*, 6662114.
92. Ding, H.; Xing, F.; Zou, L.; et al. QSAR analysis of VEGFR-2 inhibitors based on machine learning, Topomer CoMFA and molecule docking. *BMC Chem.* **2024**, *18*, 59.
93. Wang, S.; Chen, W.; Dong, C.; et al. Exploring the mechanism of genistein in treating hepatocellular carcinoma through network pharmacology and molecular docking. *Oncologie* **2024**, *26*, 799–811.
94. Kumosani, T.A.; Al-Bogami, T.J.; Barbour, E.K.; et al. Molecular docking analysis of some medicinal extracts for pro-apoptotic, antiinflammatory and antioxidative activities using HCC cell lines. *Nat. Prod. Res.* **2024**, *39*, 6665–6670.
95. Zhang, X.; Dong, P.; Song, J.; et al. Identification and mechanism prediction of mulberroside A metabolites *in vivo* and *in vitro* of rats using an integrated strategy of UHPLC-Q-Exactive Plus Orbitrap MS and network pharmacology. *Front. Chem.* **2022**, *10*, 981173.
96. Liu, Y.; Chen, M.; Chen, C.; et al. *In vitro* and *in vivo* investigation of the capacity of mulberroside A to inhibit senescence. *npj Sci. Food* **2025**, *9*, 198.
97. Naowaratwattana, W.; De-Eknamkul, W.; De Mejia, E.G. Phenolic-containing organic extracts of mulberry (*Morus alba* L.) leaves inhibit HepG2 hepatoma cells through G2/M phase arrest, induction of apoptosis, and inhibition of topoisomerase IIα activity. *J. Med. Food* **2010**, *13*, 1045–1056.
98. Boro, H.; Usha, T.; Babu, D.; et al. Hepatoprotective activity of the ethanolic extract of *Morus indica* roots from Indian Bodo tribes. *SN Appl. Sci.* **2022**, *4*, 49.
99. Kalantari, H.; Aghel, N.; Bayati, M. Hepatoprotective effect of *Morus alba* L. in carbon tetrachloride-induced hepatotoxicity in mice. *Saudi J. Gastroenterol.* **2009**, *15*, 193–197.
100. Tang, C.-C.; Huang, H.-P.; Lee, Y.-J.; et al. Hepatoprotective effect of mulberry water extracts on ethanol-induced liver injury via anti-inflammation and inhibition of lipogenesis in C57BL/6J mice. *Food Chem. Toxicol.* **2013**, *62*, 786–796.
101. Fathy, S.A.; Singab, A.N.B.; Agwa, S.A.; et al. The antiproliferative effect of mulberry (*Morus alba* L.) plant on hepatocarcinoma cell line HepG2. *Egypt. J. Med. Hum. Genet.* **2013**, *14*, 375–382.
102. Zhang, Z.; Shi, L. Anti-inflammatory and analgesic properties of cis-mulberroside A from *Ramulus mori*. *Fitoterapia* **2010**, *81*, 214–218.
103. Shal, B.; Ding, W.; Ali, H.; et al. Anti-neuroinflammatory potential of natural products in attenuation of Alzheimer's disease. *Front. Pharmacol.* **2018**, *9*, 548.
104. Eo, H.J.; Park, J.H.; Park, G.H.; et al. Anti-inflammatory and anti-cancer activity of mulberry (*Morus alba* L.) root bark. *BMC Complement. Altern. Med.* **2014**, *14*, 200.